ACS SENSORS

pubs.acs.org/acssensors Article

Nicotine Monitoring with a Wearable Sweat Band

Li-Chia Tai, Christine Heera Ahn, Hnin Yin Yin Nyein, Wenbo Ji, Mallika Bariya, Yuanjing Lin, Lu Li, and Ali Javey*

Cite This: https://dx.doi.org/10.1021/acssensors.0c00791 Read Online

ACCESS | Metrics & More | Article Recommendations | Supporting Information

ABSTRACT: The tobacco epidemic is a public health threat that has taken a heavy toll of lives around the globe each year. Smoking affects both the smokers and those who are exposed to secondhand smoke, and careful tracking of exposure can be key to mitigating the potential hazards. For smokers, the variation of chemical compositions between commercial cigarettes has led to ambiguity in estimating the health risks, both for active smokers and others involuntarily exposed to tobacco smoke and byproducts. In this regard, sweat possesses an attractive opportunity to monitor smoke exposure due to sweat's abundance in biomolecules and its great accessibility. Here, we present a wearable sweat band to monitor nicotine, a prominent ingredient in cigarettes, as a viable way to quantitatively assess a wearer's exposure to smoking. Both smokers and normal subjects are tested to demonstrate the use of this device for smoke-related health monitoring. Our results exhibit confirmable and elevated nicotine levels in sweat for subjects inhaling cigarette smoke. This continuous and personalized sweat sensing device is leverage to monitor smoke pollution for a potentially broad population.

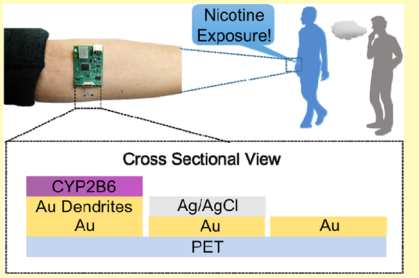

KEYWORDS: *nicotine monitoring, electrochemical devices, wearable sweat sensors, flexible electronics, nanodendrites, self-assembled monolayer*

Tobacco exposure is a leading modern-day epidemic that has claimed more than 8 million lives worldwide every year from direct tobacco use and indirect exposure to secondhand smoke.[1] These statistics convey the broad scope of people affected by smoking and the need to spearhead effective measures against smoke pollution. The adverse physiological and psychological side effects of ingredients in cigarettes can lead to sleep disorders, cardiovascular diseases, addictions, diabetes, and respiratory dysfunctions.[1−6] Therefore, tobacco smoke that permeates into various environments presents a serious public health threat that merits careful attention. The cumulative exposure to secondhand smoke in public spaces and private environments can be hard to quantify, which leads to the underestimation of irreversible health consequences on nonsmoking individuals.[7] Therefore, a tobacco-monitoring device is necessary to properly evaluate the scope of health risks among nonsmoking populations. The conventional technique to detect tobacco smoke mounts a sensor at a fixed location, which lacks the flexibility to determine smoke exposure on specific individuals and offer personalized alerts.[8] Commercially available tobacco test strips allow users to analyze urine and saliva specimens to monitor nicotine exposure at separate time points.[9] However, a test strip's inability for continuous monitoring and inconvenient processing steps make it practically challenging to capture a complete picture of an individual's exposure to tobacco and thus making efforts of tailoring preventive strategies difficult. To address the above-mentioned obstacles, we present a wearable sweat band (s-band) for nicotine monitoring to bridge the technological gap between mounted tobacco detectors and discrete nicotine testing strips. In this work, sweat is distinctively chosen as the sensing biofluid because of its abundance in biomolecules and its great accessibility.[10−17] Nicotine is selected as an attractive target due to its presence in nearly all tobacco products.[20] Like many xenobiotic biomolecules, nicotine has been demonstrated to excrete in sweat, with its concentrations positively correlated with smoking.[17−19,21] Additionally, under normal smoking conditions, sweat nicotine concentration is expected to reach up to several micromolars, which is within the detectable range with existing nicotine-sensing technologies.[17,21−25] This intimate connection between individuals' exposure to nicotine and their sweat nicotine levels provides us the framework to design a wearable s-band for nicotine monitoring. An electrochemical technique is chosen for sensor development because of its advantages for high sensitivity, good selectivity, compatibility with electronics, and low costs.[10−16] Our approach addresses the shortcomings of the current smoke-monitoring devices and paves a way to continuous, real-time, and on-site secondhand smoke monitoring. Figure 1a shows that the nicotine s-band consisted of a

Received: April 17, 2020
Accepted: May 20, 2020
Published: May 20, 2020

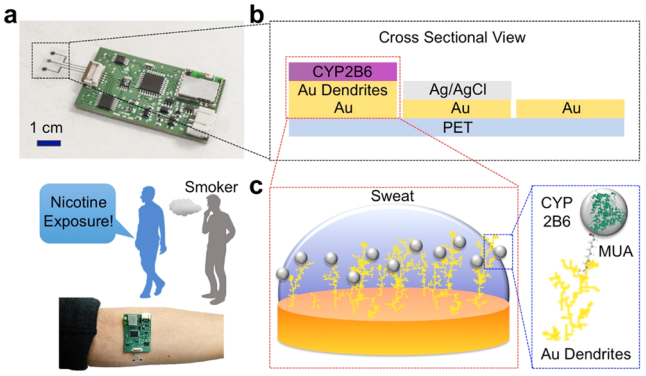

Figure 1. Design and application of the s-band. (a) Optical image of a nicotine s-band and a schematic showing the application of the wearable device on monitoring secondhand smoke. (b) A cross-sectional illustration of the flexible sensor patch, which consists of a functionalized working electrode modified with the CYP2B6 enzyme, a reference electrode pasted with silver/silver chloride, and a counter electrode. (c) Zoom-in schematics of the functionalized working electrode, which has gold nanodendrites grown on top of the gold substrate. The nanodendrites are connected to CYP2B6, a nicotine-oxidizing enzyme, via a self-assembled monolayer of 11-mercaptoundecanoic acid (MUA).

flexible electrode array connected to a compact printed circuit board. During an on-body use, the s-band is worn on the subject's forearm to detect the level of nicotine in human sweat after nicotine inhalation. The cross-sectional layers of the electrode array are shown in Figure 1b. On a poly(ethylene terephthalate) (PET) film, a gold working electrode is grown with gold nanodendrites and modified with cytochrome P450 2B6 (CYP2B6), a nicotine-oxidizing enzyme.[26−29] A silver/silver chloride reference electrode and a gold counter electrode are also integrated. Figure 1c shows a zoom-in view of the functionalized working electrode. Gold nanodendrites are directly grown on the gold electrode, and a self-assembled monolayer of 11-mercaptoundecanoic acid (MUA) is coated on top.[30,31] The MUA then immobilizes the enzyme by covalently bonding with CYP2B6.[32−34] The successful addition of each layer is supported by the electrochemical impedance spectroscopy, as shown in Figure S1.

The gold nanodendritic structure of the functionalized working electrode was captured with a scanning electron microscope (SEM), as shown in Figure 2a. The gold nanodendrites increase the surface area of the electrode to improve the sensitivity and stability of the sensor.[13,30]Figure 2b shows the oxidation peak from cyclic voltammetry (CV) of the functionalized electrode in phosphate-buffered saline (PBS) solution, with the subsequent addition of nicotine (0−30 μM). The oxidation peak increases in its height with increasing concentration of nicotine and is centered at 0.8 V, the potential chosen for amperometric testing.[22−25] For the purpose of comparison, Figure S2 shows nicotine's distinct peak relative to other xenobiotic molecules such as caffeine and levodopa. Figure 2c shows a representative plot of the amperometric response of the functionalized electrode to nicotine, and its corresponding current-to-concentration calibration curve is shown in Figure 2d. The sensitivity is calculated to be 4.3 nA/μM, which is on par with the state-of-the-art nicotine sensors.[22,23]Figure 2e shows a histogram plot of the sensor-to-sensor variation in terms of their sensitivities. The standard deviation is found to be 1.4 nA/μM, which contributes up to

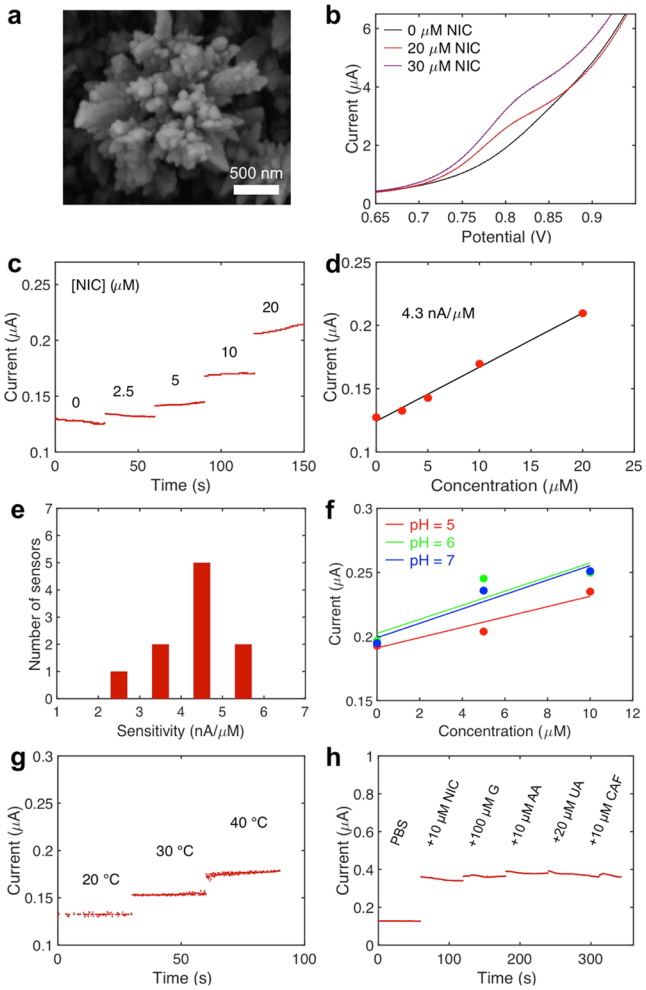

Figure 2. Characterization of the functionalized working electrode in PBS. (a) SEM image of the gold nanodendrites. (b) Zoom-in view of a CV of nicotine (NIC) dissolved in PBS. (c) Amperometric response of nicotine dissolved in PBS and (d) linear relationship of the amperometric current and nicotine concentration. (e) Sensor-to-sensor variations in terms of sensitivities. (f) Effect of pH on sensor sensitivities. (g) Effect of temperature on the amperometric response. (h) Effect of potential interferents, such as glucose (G), ascorbic acid (AA), uric acid (UA), and caffeine (CAF), on the amperometric response.

30% of deviation that dominates the linear calibration curve's uncertainty. For a high sweat nicotine level of 5 μM, this translates to about 1.6 μM of uncertainty. The effects of pH and temperature can potentially influence the performance of enzymatic-based sensors.[11]Figure 2f shows the functionalized electrode's response to varying degrees of pH, prepared using McIlvaine buffer. The range of pH (5−7) is selected in the physiologically relevant range of human sweat, and the corresponding sensitivities have a standard deviation of 0.9 nA/μM, which is within the standard deviation calculated from sensor-to-sensor variations.[11] The effect of the temperature is demonstrated in Figure 2g, where the functionalized electrode is first spiked with 5 μM of nicotine, followed by gradually increasing the temperature from 20 to 40 °C. The result shows that the sensitivity to temperature is 2.2 nA/°C, which is used to calibrate the amperometric readings prior to conversion into nicotine concentrations. The functionalized electrode's responses to interferents are tested in Figure 2h, with the

https://dx.doi.org/10.1021/acssensors.0c00791
ACS Sens. XXXX, XXX, XXX−XXX

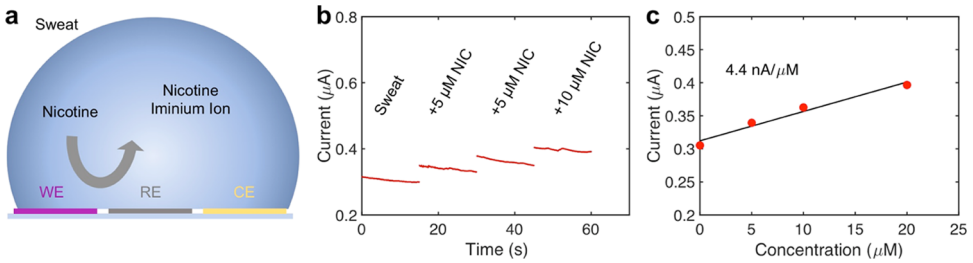

Figure 3. Characterization of the nicotine sensor in sweat solutions. (a) Sensing nicotine molecules in sweat solutions. Sweat nicotine is oxidized via CYP2B6 on the working electrode (WE) into nicotine iminium ion. The reference electrode (RE) and the counter electrode (CE) are also shown. This oxidation generates a current that is measured in terms of (b) amperometric response to nicotine. (c) Corresponding calibration curve.

addition of common biomolecules such as glucose (100 μM), ascorbic acid (10 μM), uric acid (20 μM), and caffeine (10 μM). The interferences are found to contribute to about 1 μM of uncertainty when compared to the sensor's response to nicotine.

To characterize the sensor performance in human sweat, Figure 3 shows the functionalized electrode's response in sweat solutions. Figure 3a shows a schematic of the sensing of nicotine molecules in sweat solutions, where the CYP2B6 enzyme oxidizes nicotine into nicotine iminium ion.[26−29] Figure 3b shows the amperometric response of nicotine being oxidized at a constant applied potential of 0.8 V. By adding nicotine into the sweat solution, the faradaic current increases gradually, and the current-to-concentration calibration is shown in Figure 3c. The sensitivity is found to be 4.4 nA/μM, which is similar to the sensitivity tested in PBS.

Figure 4 explores the possibility of utilizing the nicotine s-band to detect an individual's exposure to nicotine. Both

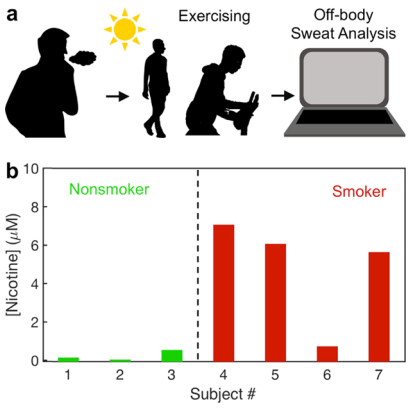

Figure 4. Nicotine monitoring via exercise-induced sweat. Sweat samples are collected after smoking (for smoking subjects) and subsequent exercise. (a) Schematics of the experiment. (b) Nicotine concentrations measured for nonsmokers and smokers.

nonsmoking subjects and smokers volunteered for this study. The subjects were permitted to generate sweat via various approaches, such as cycling, intense walking, and sports competition. Nonsmokers had no tobacco exposure, and their sweat solutions were directly analyzed after perspiration. Regular smokers started exercising within 5 min after they each smoked a standard cigarette. Their sweat solutions were similarly analyzed when they started sweating, typically 5−10 min after the start of their exercise. Figure 4a shows the experimental design using the s-band for nicotine monitoring. The subjects smoked before engaging in physical activities to generate sweat. Sweat nicotine levels were then analyzed, as described in the Experimental Section. In Figure 4b, different exercise trials, including both nonsmokers and smokers, were performed to compare the sweat nicotine levels between controls and subjects exposed to nicotine. Our results show consistently low concentrations for nonsmokers, with average nicotine levels below the limit of detection. The smokers' sweat samples exhibit elevated nicotine concentrations with an average value of 4.8 μM, which is within the concentration range previously observed.[17,21] One smoker shows a low nicotine level. This is potentially due to various factors, such as metabolic rates, the amount of nicotine content in cigarettes, and the degree of nicotine inhalation during smoking. Nevertheless, on average, we observe a good distinction of the sweat nicotine concentrations between the nonsmokers and smokers. This set of experiments demonstrates the potential for monitoring the subjects' exposure to nicotine using sweat solutions. Prior to on-body trials, the nicotine sensor is tested for a long duration, as shown in Figure S3. The signal-to-noise ratio (SNR) is calculated by dividing the change in amperometric current with the addition of 5 μM nicotine (about half of the maximum observed value of sweat nicotine concentration after regular smoking) by the amplitude of current fluctuation.[17] Based on Figure S3, the SNR is calculated to be 4, which corresponds to about 1.3 μM of uncertainty due to noise. The sensor's overall drift is small, corresponding to less than 0.16 μM/min. The detection limit is then calculated by looking at the uncertainty calculated earlier due to the interference (1 μM), sensor-to-sensor variation and linear calibration (1.6 μM), noise level (1.3 μM), and sensor drift over the average duration of on-body testing (1.3 μM) and assigning the largest value. The precision of our measurement is then constrained by the detection limit of 1.6 μM.

To demonstrate the use of the nicotine s-band for continuous nicotine monitoring, multiple subjects were recruited for sweat analysis. Figure 5a shows the experimental design with the subjects going through cycling on an ergometer. The on-body s-band seamlessly measures the nicotine level over time, with time zero indicating the start of sweating. Figure 5b shows the images of a subject cycling on an ergometer and a zoom-in view of the s-band. Two types of on-body experiments are performed. The first group includes healthy nonsmokers, and they are instructed to cycle on the ergometer for half an hour or until fatigue. As shown in Figure 5c, the nonsmokers' sweat profiles demonstrate a low nicotine concentration typically below the detection limit. Figure 5d monitors the smokers' sweat nicotine profiles. The smokers smoke one cigarette, which contains about 13 mg of nicotine, right before cycling on an ergometer.[35−37] Their sweat profiles

https://dx.doi.org/10.1021/acssensors.0c00791
ACS Sens. XXXX, XXX, XXX−XXX

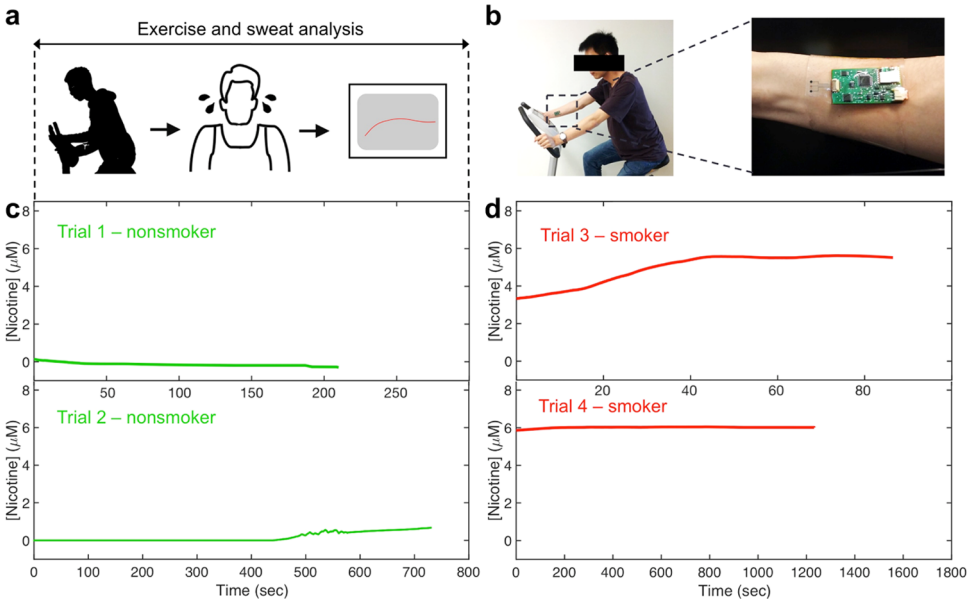

Figure 5. On-body nicotine monitoring via exercise-induced sweat. (a) Schematics of the experiment and (b) optical images of the experiment. Examples of sweat nicotine concentrations for subjects cycling on an ergometer (c) without smoking and (d) with smoking.

are then analyzed to evaluate the concentrations of nicotine. The nicotine concentrations indicate an average peak level of 5.8 μM. In both smokers' profiles, the sweat nicotine concentrations increase in the beginning, which may be attributed to the absorption of nicotine that typically happens on the order of minutes. After reaching their respective peaks, we do not observe obvious variation in their nicotine concentrations. This may be attributed to nicotine's slow metabolic decay, with the expected half-life on the order of hours.[38−40] Comparing Figure 5c,d, the distinctions between sweat profiles from smokers and nonsmokers show that the s-band can pick up the inhalation of nicotine.

In conclusion, we have demonstrated a noninvasive and wearable s-band capable of monitoring nicotine. Our work combines several layers of modification on the working electrode to allow for effective sensing. By integrating the physical properties of gold nanodendrites and the chemical bonding enabled through the self-assembled monolayers, the sensor exhibits good sensitivity and stability that are essential for detecting nicotine in sweat solutions. This amenable platform can serve as a template for future sensor designs. We have also investigated the sweat nicotine concentrations between nonsmokers and smokers, as well as their nicotine profiles over time. Our observation shows that the nicotine s-band is capable of directly picking up nicotine levels in real time for those inhaling cigarette smoke.

Importantly, the s-band overcomes the shortcomings of other commercial tobacco detectors that are limited by their lack of mobility and inability for continuous measurements. From the society's point of view, the s-band provides the general population an excellent device to monitor secondhand smoke and allows for effective policymaking related to smoke prevention. In tandem with existing sensor networks and big data analysis, the nicotine s-band can remarkably impact the healthcare industry by enriching the bioinformatics available to its users.

We envision that the nicotine s-band's long-term monitoring capability and its application geared toward the general public will significantly expand the realm of wearable sensing technologies and chart new territories for biomedical discoveries. Further, the longitudinal and cross-sectional studies enabled through the nicotine s-band will provide us with profound insight into various chronic and underlying pathological conditions that can be explored for preventive care and personalized medication.

EXPERIMENTAL SECTION

Functionalization of Electrodes to Fabricate the Nicotine Sensor. Each sensor consists of a working electrode, a reference electrode, and a counter electrode, all prepared on a PET film. The sensors were initially patterned by the photolithography technique with a positive photoresist (Shipley Microposit S1818), and chromium (30 nm) and gold (50 nm) were evaporated subsequently with the electron beam to form a conductive three-electrode system. The working electrode was modified by growing gold nanodendrites by immersing the electrode in a mixture solution of 50 mM chloroauric acid and 50 mM hydrochloric acid and applying an alternating potential via a Gamry electrochemical potentiostat (signal type: square wave; amplitude: 1 V; DC offset −1 V; signal frequency: 50 Hz; cycles: 1500). The electrodes were gently immersed in deionized water for ten seconds and left at room temperature for 2 h. Afterward, the electrodes were immersed in 11-mercaptoundecanoic acid (MUA) solution (0.5 g MUA, 1 L ethanol) for 16 h to allow self-assembled monolayers to form on top of the gold surface. Then, the electrodes were incubated in room temperature in a mixture of 1-ethyl-3-(3-dimethylaminopropyl)carbodiimide (EDC) and *N*-hydroxysuccinimide (NHS) solution (283 μL EDC, 62 mg NHS, 4 mL PBS) for 15 min. Afterward, the electrodes were incubated in a CYP2B6 enzyme solution for 1 h before drop casting the same solution on top of the working electrode (2.5 μL). The solution was prepared by mixing CYP2B6 (Sigma-Aldrich. 37.8 mg) in PBS (1 mL). The image of CYP2B6 in Figure 1 was created with www.rcsb.org.[41] The reference electrode was prepared by pasting silver/silver chloride ink onto the existing, evaporated gold electrode to provide a stable reference. The counter electrode was not modified further and remained as a simple gold electrode. The electrodes were left at room temperature overnight for the enzyme and silver/silver chloride paste to stabilize prior to testing with a potentiostat.

Nicotine Sensor's Characterization and Calibration in Buffer Solution. To characterize the functionalized working electrode, a commercial silver/silver chloride reference electrode

https://dx.doi.org/10.1021/acssensors.0c00791
ACS Sens. XXXX, XXX, XXX−XXX

and a platinum wire were used to form a complete three-electrode electrochemical system in a PBS solution. CHI 1230C potentiostat (CH Instrument) was used for electrochemical measurements. Different concentrations of nicotine were subsequently added into the solution to obtain the corresponding CV and amperometric response. The sensor's response to temperature variation was performed by heating up the nicotine solution with a hotplate and measuring the solution's temperature with a thermometer. The amperometric response was captured once the solution reached the desired temperature. The sensor's response to pH was tested in McIlvaine buffer, which had an easily tunable range of pH. The slight difference in the baseline current was normalized between McIlvaine buffer with different pH. The interference test was performed by the subsequent addition of selected categories of common biomolecules in human biofluid. The concentration of each interferent was determined to be within the normal physiological range.

Nicotine Sensor's Characterization in Sweat. The characterization of the on-body nicotine sensor in sweat solutions, as shown in Figure 3, was conducted by first collecting sweat samples from volunteers. The amperometric response of the sensor was performed by directly connecting the functionalized working, reference, and counter electrodes to the CHI 1230C potentiostat. The average value at each nicotine concentration in Figure 3b was used for plotting (Figure 3c).

Sweat Collection and Nicotine Concentration Analysis. The sweat samples were collected via various methods. Volunteers were recruited from around the City of Berkeley. Sweat was generated by intense walking, cycling (Kettler E3 Upright Exercise Bike), or playing basketball. After perspiration began, a 200 μL centrifuge tube was used to collect sweat samples from the volunteers' foreheads. The volunteers cleaned their foreheads with a gauze prior to each subsequent collection with a new centrifuge tube. Prior to testing the collected sweat samples, the nicotine sensor was characterized following the procedure described in the nicotine sensor's characterization section. Afterward, the collected sweat samples were evaluated with amperometry to convert the amperometric responses into nicotine concentrations. The institutional review board number approved at the University of California, Berkeley, is CPHS 2014-08-6636.

In Situ Sweat Nicotine Analysis. The volunteers engaged in cycling on a stationary ergometer at a biking (Kettler E3 Upright Exercise Bike) power of 100 W. The nicotine sensors, packaged in terms of the s-band, were mounted on top of the subjects' wrists over the entire duration of the cycling. The temperature calibration curve was used to convert the amperometric responses of the sensors operated at the skin temperatures of the subjects back to the current levels at room temperature, at which the sensors were characterized. The current levels were then converted to nicotine concentration using the calibration curves obtained prior to on-body exercise experiments. The raw data converted into nicotine concentration was further filtered (MATLAB Hampel Function and Smooth Function) on a personal computer.

Cigarette Smoking. The smoking subjects smoked a cigarette right before engaging in physical exercise. A standard cigarette consists of approximately 13 mg of nicotine.[35−37]

Statistical Procedures. During sensor characterization, statistical procedures were used. The sensors' sensitivities to nicotine are incorporated into a histogram plot in Figure 2e (10 sensors). The mean, median, and standard deviation are 4.4, 4.6, and 1.4 nA/μM, respectively. A representative sensor was chosen for Figure 2d, with a sensitivity of 4.3 nA/μM. In subsequent sensor characterization in Figure 3 with sweat solution, the sensor is retested for confirmation purposes if its sensitivity shows a value that is more than a standard deviation away from the statistical mean.

■ ASSOCIATED CONTENT

Supporting Information

The Supporting Information is available free of charge at https://pubs.acs.org/doi/10.1021/acssensors.0c00791.

Electrochemical impedance spectroscopy of the gold electrode under various stages of modification; oxidation peaks for selected xenobiotic molecules measured with cyclic voltammetry; long-term stability test of a functionalized working electrode (PDF)

■ AUTHOR INFORMATION

Corresponding Author

Ali Javey − *Department of Electrical Engineering and Computer Sciences and Berkeley Sensor and Actuator Center, University of California, Berkeley, California 94720, United States; Materials Science Division, Lawrence Berkeley National Laboratory, Berkeley, California 94720, United States;* orcid.org/0000-0001-7214-7931; Email: ajavey@berkeley.edu

Authors

Li-Chia Tai − *Department of Electrical Engineering and Computer Sciences and Berkeley Sensor and Actuator Center, University of California, Berkeley, California 94720, United States; Materials Science Division, Lawrence Berkeley National Laboratory, Berkeley, California 94720, United States;* orcid.org/0000-0001-7042-5109

Christine Heera Ahn − *Department of Electrical Engineering and Computer Sciences, University of California, Berkeley, California 94720, United States*

Hnin Yin Yin Nyein − *Department of Electrical Engineering and Computer Sciences and Berkeley Sensor and Actuator Center, University of California, Berkeley, California 94720, United States; Materials Science Division, Lawrence Berkeley National Laboratory, Berkeley, California 94720, United States;* orcid.org/0000-0002-5692-6182

Wenbo Ji − *Department of Electrical Engineering and Computer Sciences and Berkeley Sensor and Actuator Center, University of California, Berkeley, California 94720, United States; Materials Science Division, Lawrence Berkeley National Laboratory, Berkeley, California 94720, United States;* orcid.org/0000-0002-7913-361X

Mallika Bariya − *Department of Electrical Engineering and Computer Sciences and Berkeley Sensor and Actuator Center, University of California, Berkeley, California 94720, United States; Materials Science Division, Lawrence Berkeley National Laboratory, Berkeley, California 94720, United States;* orcid.org/0000-0002-3416-8157

Yuanjing Lin − *Department of Electrical Engineering and Computer Sciences and Berkeley Sensor and Actuator Center, University of California, Berkeley, California 94720, United States; Materials Science Division, Lawrence Berkeley National Laboratory, Berkeley, California 94720, United States;* orcid.org/0000-0002-8568-1786

Lu Li − *Department of Electrical Engineering and Computer Sciences, University of California, Berkeley, California 94720, United States; Materials Science Division, Lawrence Berkeley National Laboratory, Berkeley, California 94720, United States*

Complete contact information is available at: https://pubs.acs.org/10.1021/acssensors.0c00791

Author Contributions

L.-C.T. and A.J. designed the experiments. L.-C.T., C.H.A., and A.J. contributed to data collection, analysis, and interpretation. L.-C.T., C.H.A., H.Y.Y.N., W.J., M.B., Y.L., and L.L. contributed to sensor fabrication and preparation. L.-C.T. and A.J. wrote the paper and all authors provided feedback.

https://dx.doi.org/10.1021/acssensors.0c00791
ACS Sens. XXXX, XXX, XXX−XXX

Notes

The authors declare no competing financial interest.

■ ACKNOWLEDGMENTS

This work was supported by the National Science Foundation (NSF) Nanomanufacturing Systems for Mobile Computing and Mobile Energy Technologies (NASCENT), Berkeley Sensor and Actuator Center (BSAC), and Bakar fellowship. The sensor fabrication was performed in the Electronic Materials (E-MAT) laboratory funded by the Director, Office of Science, Office of Basic Energy Sciences, Material Sciences and Engineering Division of the U.S. Department of Energy under Contract No. DE-AC02-05CH11231.

■ REFERENCES

(1) Beaglehole, R.; Bates, C.; Youdan, B.; Bonita, R. Nicotine without Smoke: Fighting the Tobacco Epidemic with Harm Reduction. *Lancet* **2019**, *394*, 718−720.

(2) Pullan, R. D.; Rhodes, J.; Ganesh, S.; Mani, V.; Morris, J. S.; Williams, G. T.; Newcombe, R. G.; Russell, M.; Feyerabend, C.; Thomas, G.; Sawe, U. Transdermal Nicotine for Active Ulcerative Colitis. *N. Engl. J. Med.* **1994**, *330*, 811−815.

(3) Kaufman, D. W.; Helmrich, S. P.; Rosenberg, L.; Miettinen, O. S.; Shapiro, S. Nicotine and Carbon Monoxide Content of Cigarette Smoke and the Risk of Myocardial Infarction in Young Men. *N. Engl. J. Med.* **1983**, *308*, 409−413.

(4) Duncan, A.; Heyer, M. P.; Ishikawa, M.; Caligiuri, S. P. B.; Liu, X.-a.; Chen, Z.; Micioni Di Bonaventura, M. V.; Elayouby, K. S.; Ables, J. L.; Howe, W. M.; Bali, P.; Fillinger, C.; Williams, M.; O'Connor, R. M.; Wang, Z.; Lu, Q.; Kamenecka, T. M.; Ma'ayan, A.; O'Neill, H. C.; Ibanez-Tallon, I.; Geurts, A. M.; Kenny, P. J. Habenular TCF7L2 Links Nicotine Addiction to Diabetes. *Nature* **2019**, *574*, 372−377.

(5) Honein, M. A.; Rasmussen, S. A.; Reefhuis, J.; Romitti, P. A.; Lammer, E. J.; Sun, L.; Correa, A. Maternal Smoking and Environmental Tobacco Smoke Exposure and the Risk of Orofacial Clefts. *Epidemiology* **2007**, *18*, 226−233.

(6) Popa, C. Breathing Disorders Using Photoacoustics Gas Analyzer. *J. Med. Imaging Health Inf.* **2016**, *6*, 1893−1895.

(7) Coultas, D. B.; Howard, C. A.; Peake, G. T.; Skipper, B. J.; Samet, J. M. Salivary Cotinine Levels and Involuntary Tobacco Smoke Exposure in Children and Adults in New Mexico. *Am. Rev. Respir. Dis.* **1987**, *136*, 305−309.

(8) Liu, Y.; Antwi-Boampong, S.; BelBruno, J. J.; Crane, M. A.; Tanski, S. E. Detection of Secondhand Cigarette Smoke via Nicotine Using Conductive Polymer Films. *Nicotine Tob. Res.* **2013**, *15*, 1511−1518.

(9) Achilihu, H.; Feng, J.; Wang, L.; Bernert, J. T. Tobacco Use Classification by Inexpensive Urinary Cotinine Immunoassay Test Strips. *J. Anal. Toxicol.* **2019**, *43*, 149−153.

(10) Tai, L.-C.; Gao, W.; Chao, M.; Bariya, M.; Ngo, Q. P.; Shahpar, Z.; Nyein, H. Y. Y.; Park, H.; Sun, J.; Jung, Y.; Wu, E.; Fahad, H. M.; Lien, D.-H.; Ota, H.; Cho, G.; Javey, A. Methylxanthine Drug Monitoring with Wearable Sweat Sensors. *Adv. Mater.* **2018**, *30*, No. 1707442.

(11) Gao, W.; Emaminejad, S.; Nyein, H. Y. Y.; Challa, S.; Chen, K.; Peck, A.; Fahad, H. M.; Ota, H.; Shiraki, H.; Kiriya, D.; Lien, D.-H.; Brooks, G. A.; Davis, R. W.; Javey, A. Fully Integrated Wearable Sensor Arrays for Multiplexed in Situ Perspiration Analysis. *Nature* **2016**, *529*, 509−514.

(12) Emaminejad, S.; Gao, W.; Wu, E.; Davies, Z. A.; Yin Yin Nyein, H.; Challa, S.; Ryan, S. P.; Fahad, H. M.; Chen, K.; Shahpar, Z.; Talebi, S.; Milla, C.; Javey, A.; Davis, R. W. Autonomous Sweat Extraction and Analysis Applied to Cystic Fibrosis and Glucose Monitoring Using a Fully Integrated Wearable Platform. *Proc. Natl. Acad. Sci. U.S.A.* **2017**, *114*, 4625−4630.

(13) Tai, L.-C.; Liaw, T. S.; Lin, Y.; Nyein, H. Y. Y.; Bariya, M.; Ji, W.; Hettick, M.; Zhao, C.; Zhao, J.; Hou, L.; Yuan, Z.; Fan, Z.; Javey, A. Wearable Sweat Band for Noninvasive Levodopa Monitoring. *Nano Lett.* **2019**, *19*, 6346−6351.

(14) Nyein, H. Y. Y.; Bariya, M.; Kivimäki, L.; Uusitalo, S.; Liaw, T. S.; Jansson, E.; Ahn, C. H.; Hangasky, J. A.; Zhao, J.; Lin, Y.; Happonen, T.; Chao, M.; Liedert, C.; Zhao, Y.; Tai, L.-C.; Hiltunen, J.; Javey, A. Regional and Correlative Sweat Analysis Using High-throughput Microfluidic Sensing Patches Toward Decoding Sweat. *Sci. Adv.* **2019**, *5*, No. eaaw9906.

(15) Kim, J.; Jeerapan, I.; Imani, S.; Cho, T. N.; Bandodkar, A.; Cinti, S.; Mercier, P. P.; Wang, J. Noninvasive Alcohol Monitoring Using a Wearable Tattoo-Based Iontophoretic-Biosensing System. *ACS Sens.* **2016**, *1*, 1011−1019.

(16) Krishnan, S. R.; Ray, T. R.; Ayer, A. B.; Ma, Y.; Gutruf, P.; Lee, K.; Lee, J. Y.; Wei, C.; Feng, X.; Ng, B.; Abecassis, Z. A.; Murthy, N.; Stankiewicz, I.; Freudman, J.; Stillman, J.; Kim, N.; Young, G.; Goudeseune, C.; Ciraldo, J.; Tate, M.; Huang, Y.; Potts, M.; Rogers, J. A. Epidermal Electronics for Noninvasive, Wireless, Quantitative Assessment of Ventricular Shunt Function in Patients with Hydrocephalus. *Sci. Transl. Med.* **2018**, *10*, No. eaat8437.

(17) Kintz, P.; Henrich, A.; Cirimele, V.; Ludes, B. Nicotine Monitoring in Sweat with a Sweat Patch. *J. Chromatogr. B: Biomed. Sci. Appl.* **1998**, *705*, 357−361.

(18) Tsunoda, M.; Hirayama, M.; Tsuda, T.; Ohno, K. Noninvasive Monitoring of Plasma L-dopa Concentrations Using Sweat Samples in Parkinson's Disease. *Clin. Chim. Acta* **2015**, *442*, 52−55.

(19) Kovacs, E. M. R.; Stegen, J. H. C. H.; Brouns, F. Effect of Caffeinated Drinks on Substrate Metabolism, Caffeine Excretion, and Performance. *J. Appl. Physiol.* **1998**, *85*, 709−715.

(20) Stanfill, S. B.; Connolly, G. N.; Zhang, L.; Jia, L. T.; Henningfield, J. E.; Richter, P.; Lawler, T. S.; Ayo-Yusuf, O. A.; Ashley, D. L.; Watson, C. H. Global surveillance of oral tobacco products: total nicotine, unionised nicotine and tobacco-specific N-nitrosamines. *Tob. Control* **2011**, *20*, No. e2.

(21) Henningfield, J. E.; Stapleton, J. M.; Benowitz, N. L.; Grayson, R. F.; London, E. D. Higher Levels of Nicotine in Arterial than in Venous Blood after Cigarette Smoking. *Drug Alcohol Depend.* **1993**, *33*, 23−29.

(22) Jing, Y.; Yuan, X.; Yuan, Q.; He, K.; Liu, Y.; Lu, P.; Li, H.; Li, B.; Zhan, H.; Li, G. Determination of Nicotine in Tobacco Products Based on Mussel-inspired Reduced Graphene Oxide-supported Gold Nanoparticles. *Sci. Rep.* **2016**, *6*, No. 29230.

(23) Goodarzi, Z.; Maghrebi, M.; Zavareh, A. F.; Mokhtari-Hosseini, Z.-B.; Ebrahimi-hoseinzadeh, B.; Zarmi, A. H.; Barshan-tashnizi, M. Evaluation of Nicotine Sensor Based on Copper Nanoparticles and Carbon Nanotubes. *J. Nanostruct. Chem.* **2015**, *5*, 237−242.

(24) Fekry, A. M.; Azab, S. M.; Shehata, M.; Ameer, M. A. A Novel Electrochemical Nicotine Sensor Based on Cerium Nanoparticles with Anionic Surfactant. *RSC Adv.* **2015**, *5*, 51662−51671.

(25) Stočes, M.; Švancara, I. Electrochemical Behavior of Nicotine at Unmodified Carbon Paste Electrode and Its Determination in a Set of Refilling Liquids for Electronic Cigarettes. *Electroanalysis* **2014**, *26*, 2655−2663.

(26) Hecht, S. S.; Hochalter, J. B.; Villalta, P. W.; Murphy, S. E. 2′-Hydroxylation of Nicotine by Cytochrome P450 2A6 and Human Liver Microsomes: Formation of a Lung Carcinogen Precursor. *Proc. Natl. Acad. Sci. U.S.A.* **2000**, *97*, 12493−12497.

(27) Bloom, A. J.; Wang, P.-F.; Kharasch, E. D. Nicotine Oxidation by Genetic Variants of CYP2B6 and in Human Brain Microsomes. *Pharmacol. Res. Perspect.* **2019**, *7*, No. e00468.

(28) Yamazaki, H.; Inoue, K.; Hashimoto, M.; Shimada, T. Roles of CYP2A6 and CYP2B6 in Nicotine C-oxidation by Human Liver Microsomes. *Arch. Toxicol.* **1999**, *73*, 65−70.

(29) Dicke, K. E.; Skrlin, S. M.; Murphy, S. E. Nicotine and 4-(methylnitrosamino)-1-(3-pyridyl)-butanone Metabolism by Cytochrome P450 2B6. *Drug Metab. Dispos.* **2005**, *33*, 1760−1764.

(30) Lin, Y.; Bariya, M.; Nyein, H. Y. Y.; Kivimäki, L.; Uusitalo, S.; Jansson, E.; Ji, W.; Yuan, Z.; Happonen, T.; Liedert, C.; Hiltunen, J.;

https://dx.doi.org/10.1021/acssensors.0c00791
ACS Sens. XXXX, XXX, XXX−XXX

Fan, Z.; Javey, A. Porous Enzymatic Membrane for Nanotextured Glucose Sweat Sensors with High Stability toward Reliable Non-invasive Health Monitoring. *Adv. Funct. Mater.* **2019**, *29*, No. 1902521.
(31) Kamra, T.; Chaudhary, S.; Xu, C.; Montelius, L.; Schnadt, J.; Ye, L. Covalent Immobilization of Molecularly Imprinted Polymer Nanoparticles on a Gold Surface Using Carbodiimide Coupling for Chemical Sensing. *J. Colloid Interface Sci.* **2016**, *461*, 1−8.
(32) Fantuzzi, A.; Fairhead, M.; Gilardi, G. Direct Electrochemistry of Immobilized Human Cytochrome P450 2E1. *J. Am. Chem. Soc.* **2004**, *126*, 5040−5041.
(33) Alonso-Lomillo, M. A.; Yardimci, C.; Domínguez-Renedo, O.; Arcos-Martínez, M. J. CYP450 2B4 Covalently Attached to Carbon and Gold Screen Printed Electrodes by Diazonium Salt and Thiols Monolayers. *Anal. Chim. Acta* **2009**, *633*, 51−56.
(34) Peng, L.; Yang, X.; Zhang, Q.; Liu, S. Electrochemistry of Cytochrome P450 2B6 on Electrodes Modified with Zirconium Dioxide Nanoparticles and Platin Components. *Electroanalysis* **2008**, *20*, 803−807.
(35) Hatsukami, D. K.; Hertsgaard, L. A.; Vogel, R. I.; Jensen, J. A.; Murphy, S. E.; Hecht, S. S.; Carmella, S. G.; al'Absi, M.; Joseph, A. M.; Allen, S. S. Reduced Nicotine Content Cigarettes and Nicotine Patch. *Cancer Epidemiol., Biomarkers Prev.* **2013**, *22*, 1015−1024.
(36) Benowitz, N. L.; Dains, K. M.; Hall, S. M.; Stewart, S.; Wilson, M.; Dempsey, D.; Jacob, P., III Smoking Behavior and Exposure to Tobacco Toxicants during 6 Months of Smoking Progressively Reduced Nicotine Content Cigarettes. *Cancer Epidemiol., Biomarkers Prev.* **2012**, *21*, 761−769.
(37) Bullen, C.; Howe, C.; Laugesen, M.; McRobbie, H.; Parag, V.; Williman, J.; Walker, N. Electronic Cigarettes for Smoking Cessation: a Randomised Controlled Trial. *Lancet* **2013**, *382*, 1629−1637.
(38) Benowitz, N. L.; Porchet, H.; Sheiner, L.; Jacob, P. Nicotine Absorption and Cardiovascular Effects with Smokeless Tobacco Use: Comparison with Cigarettes and Nicotine Gum. *Clin. Pharmacol. Ther.* **1988**, *44*, 23−28.
(39) Bernert, J. T.; Alexander, J. R.; Sosnoff, C. S.; McGuffey, J. E. Time Course of Nicotine and Cotinine Incorporation into Samples of Nonsmokers' Beard Hair Following a Single Dose of Nicotine Polacrilex. *J. Anal. Toxicol.* **2011**, *35*, 1−7.
(40) Yingst, J. M.; Foulds, J.; Veldheer, S.; Hrabovsky, S.; Trushin, N.; Eissenberg, T. T.; Williams, J.; Richie, J. P.; Nichols, T. T.; Wilson, S. J.; Hobkirk, A. L. Nicotine Absorption during Electronic Cigarette Use among Regular Users. *PLoS One* **2019**, *14*, No. e0220300.
(41) Berman, H. M.; Westbrook, J.; Feng, Z.; Gilliland, G.; Bhat, T. N.; Weissig, H.; Shindyalov, I. N.; Bourne, P. E. The Protein Data Bank. *Nucleic Acids Res.* **2000**, *28*, 235−242.

https://dx.doi.org/10.1021/acssensors.0c00791
ACS Sens. XXXX, XXX, XXX−XXX